

Nanocrystalline zinc oxide in perfluorinated ionomer membranes: Preparation, characterization, and photocatalytic properties

Jianchun Wang, Ping Liu, Shiming Wang, Wei Han, Xuxu Wang, Xianzhi Fu*

Research Institute of Photocatalysis, Chemistry & Chemical Engineering College, Fuzhou University, Fuzhou 350002, China

Received 5 February 2007; received in revised form 22 March 2007; accepted 22 March 2007

Available online 27 March 2007

Abstract

Crystalline ZnO nanoparticles were synthesized via the templating method by taking advantage of the hydrophilic cavities of the Nafion ionomer membranes. The ZnO-embedded Nafion film was characterized by various methods, including optical absorption, X-ray diffraction and high-resolution transmission electron microscopy. The film was of high optical quality, and exhibited excellent photocatalytic activity toward rhodamine B degradation under UV irradiation. Unlike unprotected bulk ZnO nanocrystals, the ZnO nanocatalysts embedded in Nafion membranes were found to be highly stable against photocorrosion, with hardly any reduction in the activity even after 10 times of repeated reaction cycles. The implications of the results are discussed.

© 2007 Elsevier B.V. All rights reserved.

Keywords: ZnO; Nafion; Photocatalysis; Rhodamine B; Photocorrosion

1. Introduction

Zinc oxide (ZnO) is a well-known semiconductor with a wide band gap and high exciton binding energy at room temperature. It is one of the most important functional inorganic materials with unique catalytic [1,2], electrical [3,4], optoelectronic [5,6], and photochemical [7] properties, stimulating wide research interest in its potential applications. The use of ZnO semiconductor for photocatalytic degradation of environmental pollutants was believed to be advantageous over other materials due to its non-toxic nature, low cost, and high reactivity [8,9]. However, the photocorrosion of ZnO in such applications has been a significant issue [10,11].

Perfluorinated ionomer membranes, such as Nafion, are widely used in the fields of electrochemistry and catalysis, such as the plating industry, surface treatment of metals, batteries, sensors, drug release, fuel cells, catalysts and so on [12–17]. The Nafion membrane is also excellent support for semiconductor nanocrystals because of the superior chemical stability, high

mechanical strength, and high optical quality. The hydrophilic cavities in the perfluorinated ionomer membranes are convenient templates for the nanoparticle formation. For example, nanoscale ZnS [18], CdS [19,20], PbS [21], Ag₂S [22], Fe₂O₃ [23], SiO₂ [24], and TiO₂ [25] have all been synthesized by using this method. There are several distinct advantages for the Nafion-templating approach. First, the Nafion membrane provides a stable matrix to prevent the agglomeration and corrosion of the nanoparticles embedded [25,26]. Second, the nanoparticles embedded in Nafion membrane are easy to handle and recycle for catalytic purposes [26,27]. Third, Nafion membranes have low absorbance in the UV–vis region, and their hydrophilic cavities and channels possess strong polarity and excellent ion-exchange properties. These characteristics may enhance the adsorptive capacity of the materials, leading to the enrichment of pollutants on the surface of catalytic nanoparticles in water.

In this work, we report the synthesis of crystalline ZnO nanoparticles in Nafion membranes by using the templating method. The ZnO-embedded Nafion film was characterized by many instrumental methods, supporting the nanoscale nature of the embedded ZnO species. The film showed excellent photocatalytic properties with the activity being stable over multiple repeated uses.

* Corresponding author. Fax: +86 591 83738608.
E-mail address: xzfu@fzu.edu.cn (X. Fu).

2. Experimental

2.1. Materials

Zinc nitrate, sodium hydroxide, and rhodamine B were purchased from Shanghai Chemical Reagents Company. All chemicals were of analytical purity and used as received. Water was deionized and purified by passing through a water purification system.

Nafion-117 membranes (equivalent mass $\sim 1100 \text{ g mol}^{-1}$) were purchased from DuPont Company. A membrane sample (thickness $\sim 0.178 \text{ mm}$) was cut into small pieces of suitable sizes and purified to remove colored impurities by following an established procedure [28]. Briefly, the membrane pieces were immersed sequentially in concentrated (70%), 60%, 40%, and 20% nitric acid at 60°C for 24, 2, 2, and 2 h, respectively, followed by thoroughly rinsing with deionized water until neutral. The purified membrane samples were colorless and optically transparent down to 230 nm, and were kept fully hydrated before use.

2.2. Preparation of ZnO-Nafion membrane

In a typical experiment, a piece of purified Nafion membrane film ($1.5 \text{ cm} \times 6 \text{ cm}$) was soaked in an aqueous solution of zinc nitrate (50 mL , 0.5 mol L^{-1}) overnight. The film was then thoroughly rinsed and immersed in deionized water for 24 h, and soaked in an ethanol solution of sodium hydroxide (50 mL , 0.5 mol L^{-1}) for 30 min at room temperature with stirring. After again thorough rinsing and immersing in deionized water for 24 h, a light-blue-colored ZnO-embedded Nafion sample (ZnO-Nafion) was obtained.

2.3. Photocatalytic activity measurements

The experimental set-up is shown in Fig. 1. The quartz photoreactor was designed in the shape of a column (100 mm in length and 16 mm in diameter). Deionized water was passed through the quartz jacket to maintain the reaction temperature

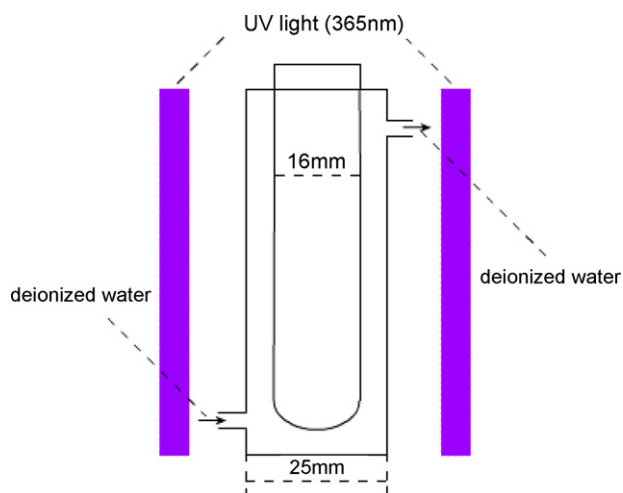


Fig. 1. The experimental set-up for photocatalytic activity.

($25 \pm 1.0^\circ\text{C}$) as well as UV transparency for the reactor. The reactor was illuminated by four surrounding UV lamps (4 W, Philips TL/05) which predominantly emit at 365 nm.

The photocatalytic activities of the membrane film samples were assessed by monitoring the decomposition rate of RhB. In a typical reaction, a piece of ZnO-Nafion membrane film was first immersed in an aqueous RhB solution ($1.0 \times 10^{-5} \text{ mol L}^{-1}$, 20 mL) in the dark for $\sim 18 \text{ h}$ to establish the adsorption equilibrium. The amount (in grams) of RhB adsorbed in the membrane was calculated by the following equation: $m = MV(C_0 - C_t)$, where C_0 is the initial concentration of RhB solution, C_t the final concentration left in RhB solution, M the molecular weight of RhB, and V is the volume of RhB solution used. C_0 and C_t were calculated according to the absorbance at 554 nm of the solution and known extinction coefficient of RhB. The film was then placed into the reactor full of deionized water, and irradiated by UV light. The change of RhB absorbance in the membrane was used to monitor the extent of reaction at given irradiation time intervals.

2.4. Characterizations

X-ray diffraction (XRD) patterns were collected on a Bruker D8 Advance X-ray diffractometer with Cu $K\alpha$ radiation operated at 40 kV and 40 mA. The data were recorded in the 2θ range of $25\text{--}70^\circ$ with a step width of 0.02° and counting time of 5 s for improved signal-to-noise ratio. The high-resolution transmission electron microscopy (HR-TEM) images were obtained on an FEI TECNAI G² F20 microscope at an accelerating voltage of 200 kV. UV-vis absorption spectra were recorded on a Cary-500 UV-vis-NIR spectrophotometer. Atomic absorption analysis was carried out on a Varian Model SpectraAA-220 atomic absorption spectrophotometer with a deuterium background corrector and an 11-mA hollow cathode lamp.

3. Results and discussion

3.1. Preparation and characterization

The preparation of the ZnO-Nafion membrane film was based on a traditional strategy for the formation of nanoparticles by using the hydrophilic cavities of Nafion as templates [23,26]. Blank-Nafion was soaked in aqueous zinc nitrate solution overnight to facilitate Zn^{2+} ion exchange. The Zn^{2+} -Nafion was then soaked in sodium hydroxide ethanol solution to introduce the hydroxide. Here, the ethanol solution swelled the membrane film and made the entrance of hydroxide become easily and uniformly.

The obtained ZnO-Nafion membrane film is also transparent (similar to Blank-Nafion), but with a light blue color, serving as a visual indication for the presence of foreign species (ZnO) in the Nafion film. Consistently, in the optical absorption spectrum of the ZnO-Nafion film (Fig. 2), the absorption threshold is at $\sim 350 \text{ nm}$, in comparison to $\sim 230 \text{ nm}$ for Blank-Nafion. In addition, the absorption threshold for the ZnO-Nafion film is somewhat blue shifted in comparison to those of large-sized ZnO particles ($\sim 380 \text{ nm}$ [29]), indicating that there might be quan-

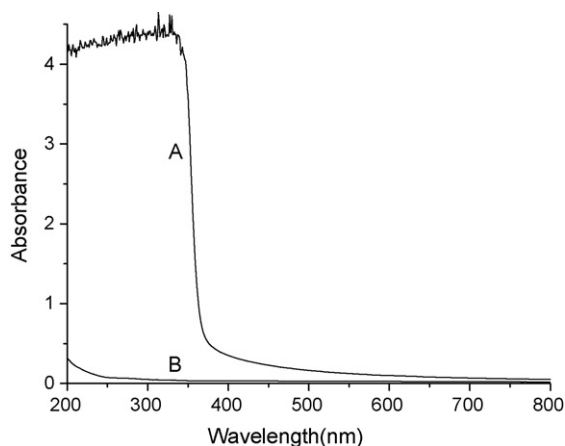


Fig. 2. UV-vis absorption spectra of ZnO-Nafion (curve A) and Blank-Nafion (curve B).

tum confinement effect likely due to the presence of nanosized ZnO species.

The XRD patterns of the ZnO-Nafion film (Fig. 3) showed multiple diffraction peaks over a broad Nafion background (peak at $\sim 39^\circ$). The peaks were found at $2\theta \sim 31.7^\circ$, 34.4° , 36.2° , 47.5° , 56.5° , 62.8° , and 67.9° , which could be readily assigned to (100), (002), (101), (102), (110), (103), and (112) lattice planes of hexagonal ZnO crystal (JCPDS 89-1397), respectively. These peaks are rather broad, indicating that ZnO crystals existed with nanosize, which was consistent with the result obtained from the HR-TEM measurements.

The presence of ZnO nanocrystals was further confirmed by HR-TEM studies. For the analysis, the ZnO-Nafion film was microtomed to obtain ultrathin (70–90 nm) cross-sectional slices, which were placed onto carbon-coated copper grids to be ready for imaging. Abundant well-dispersed nanosized ZnO particles were found in the specimens. The average size for the nanoparticles was calculated to be 8 nm. The lattice fringes of the ZnO nanocrystals could be clearly observed. For example, as shown in Fig. 4, the individual spacing for the nanocrystal was measured to be 0.192 nm, in agreement with the (102) plane of hexagonal ZnO.

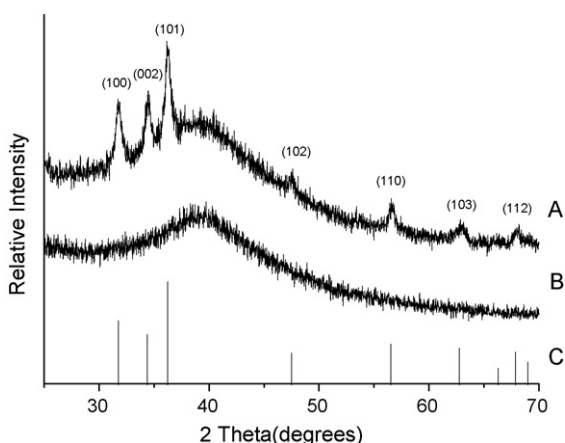


Fig. 3. X-ray diffraction patterns of (A) ZnO-Nafion, (B) Blank-Nafion, and (C) ZnO from the JCPDS database.

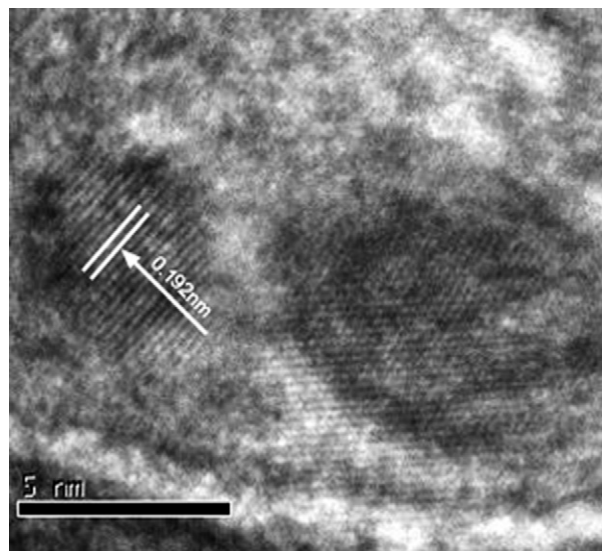


Fig. 4. High-resolution TEM image of ZnO-Nafion.

3.2. RhB adsorption and photocatalytic degradation

After 18 h in the dark, the adsorption equilibrium of RhB in the membrane was reached. Most of the RhB were adsorbed in the Blank-Nafion and ZnO-Nafion films, and only 16.82% and 18.74% of RhB left in the solution. In other words, there were 0.080 mg and 0.077 mg of RhB in the Blank-Nafion and ZnO-Nafion, respectively. Due to the ZnO nanoparticles embedded in the Nafion membrane, the amount of RhB adsorbed in ZnO-Nafion was somewhat decreased, as compared to the adsorption in Blank-Nafion.

The RhB-adsorbed Nafion membrane films exhibit typical absorption features due to RhB. As presented in Fig. 5, the RhB-adsorbed ZnO-Nafion film showed maximum absorption at 547 nm (curve A), while that for the Blank-Nafion is at 554 nm (curve B). Similar blue shifts of RhB absorption band (K band) were also observed when lower the solvent polarity in solutions [30,31], which might share similar mechanistic origin to that in the ZnO-Nafion film vs. Blank-Nafion film. More specifically,

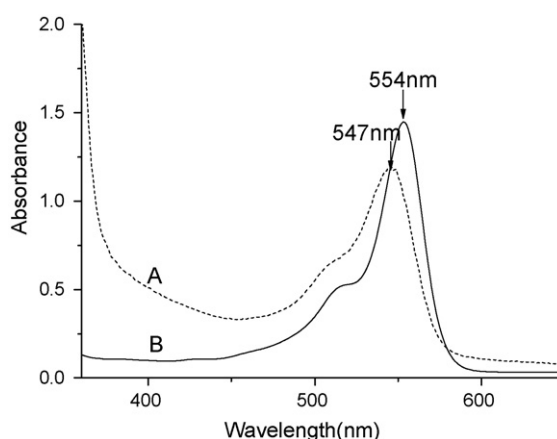


Fig. 5. A typical absorption spectra of Nafion membrane with rhodamine B: (A) ZnO-Nafion for 18 h; (B) Blank-Nafion for 18 h.

the blue shift of RhB absorption peak in the presence of ZnO could be attributed to the less polarizable excited state (π^*) than the ground state (π). Thus, there are smaller attractive (van der Waals) forces with larger system volume [31,32].

The progress of the UV (365 nm) photodegradation reaction of RhB was monitored by the change of corresponding RhB absorption maximum. As shown in Fig. 6a, the RhB absorption in decreased $\sim 90.6\%$ for the ZnO-Nafion film (curve B) in the entire course of UV irradiation (210 min), while it hardly changed at all for the Blank-Nafion film (curve A). This result indicates that ZnO nanoparticles in the Nafion film are excellent photocatalysts for RhB degradation under the experimental conditions.

Watanabe et al. [30] used CdS as a photocatalyst to study the photodegradation mechanism of RhB, and they found that the absorption maximum of RhB solution shifted from 555 to 498 nm. Liquid chromatograph analysis showed that the intermediates were rhodamine B, TER, DER, MER, and rhodamine, respectively. The mechanism was further reconfirmed by Ma and Yao [33] using anatase TiO₂ film as the photocatalyst. Besides, they used the film coated by P-25 as the photocatalyst and found another mechanism of photodegradation of RhB. Similar work was also done by other researchers. Here, the progressive spectral changes of RhB adsorbed in ZnO-Nafion upon

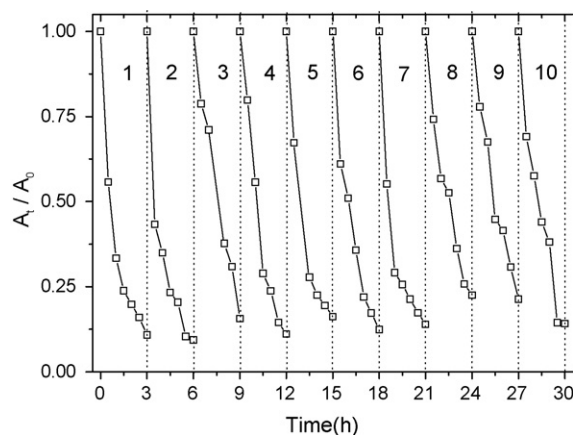


Fig. 7. Cyclic photodegradation of RhB under UV light for 10 times.

UV irradiation (Fig. 6b) showed the progressive decrease of spectral intensity (hardly observable after 210 min), indicating that the chromophoric structure of RhB was destroyed. No RhB was detected in the deionized water during and after the photoreaction, suggesting that there was no solute leach from the membrane. However, there was neither any peak shift nor the appearance of any new peak, strongly suggesting that the lack of *N*-de-ethylation process which is common in P25 photocatalytic systems for RhB degradation [33,34].

Unlike traditional ZnO photocatalysts [11,35,36], the ZnO nanoparticles embedded in Nafion films are quite stable against photocorrosion, a common property shared by many nanocatalysts encapsulated in Nafion [25–27]. This allowed the convenient recycling of the catalysts with little reduction in their photocatalytic activity even after repeated uses [26]. As shown in Fig. 7, the ZnO-Nafion film exhibited remarkable photostability without any appreciable loss of photocatalytic activity even after 10 cycles. Such stability was further supported by the atomic absorption analysis results. For example, the concentration of Zn²⁺ ions in the solution mixture after photoreaction (3 h) was measured to be $\sim 0.0148 \text{ mg L}^{-1}$ for the ZnO-Nafion film, while the value was $\sim 0.2318 \text{ mg L}^{-1}$ when commercial bulk ZnO nanocrystals (average $\sim 59.8 \text{ nm}$) of the same mass was used.

4. Conclusions

Crystalline ZnO nanoparticles were synthesized via the templating method by taking advantage of the hydrophilic cavities of the Nafion ionomer membranes. The ZnO-Nafion film was characterized by various methods, including optical absorption, XRD and HR-TEM. The film was of high optical quality, and exhibited excellent photocatalytic activity toward rhodamine B degradation under UV irradiation. Unlike unprotected bulk ZnO nanocrystals, the ZnO nanocatalysts embedded in Nafion membranes were found to be highly stable against photocorrosion, with hardly any reduction in their activity even after 10 repeated reaction cycles. Such robust ZnO-Nafion membrane films might find unique applications in photocatalytic reactions.

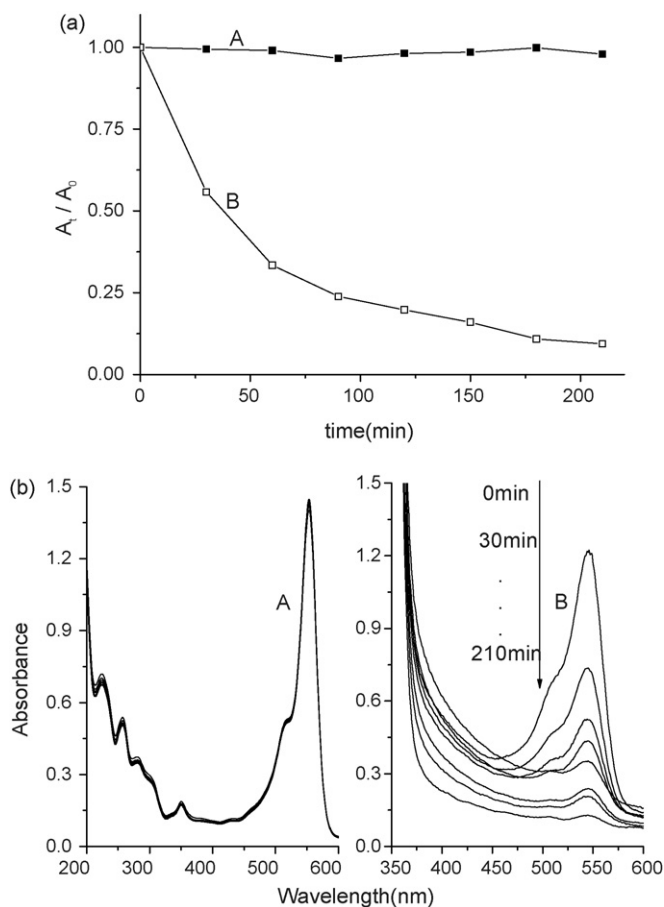


Fig. 6. (a) Degradation of rhodamine B by UV light (365 nm): (A) Blank-Nafion; (B) ZnO-Nafion. (b) The progressive spectral changes of RhB upon UV light (365 nm) irradiation: (A) Blank-Nafion; (B) ZnO-Nafion.

Acknowledgments

This work was financially supported by the National Natural Science Foundation of China (nos. 20473017, 20537010, and 20573020), and the National Key Basic Research Special Foundation (2004CCA07100). The authors are indebted to Dr. Yi Lin at Clemson University for his instructive comment and kind help on preparing this paper.

References

- [1] A. Music, J. Batista, J. Levec, *Appl. Catal. A* 165 (1997) 115–131.
- [2] S.A. French, A.A. Sokol, S.T. Bromley, C.R.A. Catlow, P. Sherwood, *Top. Catal.* 24 (2003) 161–172.
- [3] D.H. Zhang, T.L. Yang, Q.P. Wang, D.J. Zhang, *Mater. Chem. Phys.* 68 (2001) 233–238.
- [4] D.C. Look, C. Coskun, B. Claffin, G.C. Farlow, *Phys. B: Condens. Matter* 340 (2003) 32–38.
- [5] M. Purica, E. Budianu, E. Rusu, *Microelectron. Eng.* 51–2 (2000) 425–431.
- [6] C.C. Lin, H.P. Chen, S.Y. Chen, *Chem. Phys. Lett.* 404 (2005) 30–34.
- [7] M. Schubnell, I. Kamber, P. Beaud, *Appl. Phys. A: Mater. Sci. Process.* 64 (1997) 109–113.
- [8] A. Akyol, H.C. Yatmaz, M. Bayramoglu, *Appl. Catal. B* 54 (2004) 19–24.
- [9] S. Chakrabarti, B.K. Dutta, *J. Hazard. Mater.* 112 (2004) 269–278.
- [10] P. Spathis, I. Poulos, *Corros. Sci.* 37 (1995) 673–680.
- [11] M.R. Hoffmann, S.T. Martin, W.Y. Choi, D.W. Bahnemann, *Chem. Rev.* 95 (1995) 69–96.
- [12] C. Heitner Wirguin, *J. Membr. Sci.* 120 (1) (1996) 1–33.
- [13] J. Fenandez, J. Bandara, A. Lopez, P. Albers, J. Kiwi, *Chem. Commun.* (1998) 1493–1494.
- [14] J. Fenandez, J. Bandara, A. Lopez, Ph. Buffat, J. Kiwi, *Langmuir* 15 (1999) 185–192.
- [15] J. Kiwi, M.R. Dhananjeyan, V. Nadtochenko, *J. Phys. Chem. A* 106 (31) (2002) 7138–7146.
- [16] J. Kiwi, N. Denisov, Y. Gak, N. Ovanesyan, P.A. Buffat, E. Suvorova, F. Gostev, A. Titov, O. Sarkisov, P. Albers, V. Nadtochenko, *Langmuir* 18 (23) (2002) 9054–9066.
- [17] S. Parra, L. Henao, E. Mielczarski, J. Mielczarski, P. Albers, E. Suvorova, J. Guindet, J. Kiwi, *Langmuir* 20 (2004) 5621–5629.
- [18] M.F. Finlayson, K.H. Park, N. Kakuta, A.J. Bard, A. Campion, M.A. Fox, S.E. Webber, J.M. White, *J. Lumin.* 39 (1988) 205–214.
- [19] N. Kakuta, J.M. White, A. Campion, A.J. Bard, M.A. Fox, S.E. Webber, *J. Phys. Chem.* 89 (1985) 48–52.
- [20] P. Nandakumar, C. Vijayan, K. Dhanalakshmi, G. Sundararajan, P.K. Nair, Y.V.G.S. Murti, *Mater. Sci. Eng. B* 83 (2001) 61–65.
- [21] H. Miyoshi, M. Yamachika, H. Yoneyama, H. Mori, *J. Chem. Soc., Faraday Trans.* 86 (1990) 815–818.
- [22] H.W. Rollins, F. Lin, J. Johnson, J.J. Ma, J.T. Liu, M.H. Tu, D.D. Des-Marteau, Y.P. Sun, *Langmuir* 16 (2000) 8031–8036.
- [23] L. Raymond, J.F. Revol, D.H. Ryan, R.H. Marchessault, *J. Appl. Polym. Sci.* 59 (1996) 1073–1086.
- [24] P.L. Shao, K.A. Mauritz, R.B. Moore, *J. Polym. Sci., Part B: Polym. Phys.* 34 (1996) 873–882.
- [25] P. Liu, J. Bandara, Y. Lin, D. Elgin, L.F. Allard, Y.P. Sun, *Langmuir* 18 (2002) 10398–10401.
- [26] S.M. Wang, P. Liu, X.X. Wang, X.Z. Fu, *Langmuir* 21 (2005) 11969–11973.
- [27] P. Pathak, M.J. Meziani, Y. Li, L.T. Cureton, Y.P. Sun, *Chem. Commun.* (2004) 1234–1235.
- [28] C.E. Bunker, H.W. Rollins, B. Ma, K.J. Simmons, J.T. Liu, J.J. Ma, C.W. Martin, D.D. DesMarteau, Y.P. Sun, *J. Photochem. Photobiol. A* 126 (1999) 71–76.
- [29] G. Ramakrishna, H.N. Ghosh, *Langmuir* 19 (2003) 3006–3012.
- [30] T. Watanabe, T. Takizawa, K. Honda, *J. Phys. Chem.* 81 (1977) 1845–1851.
- [31] A.D. Stein, M.D. Fayer, *J. Chem. Phys.* 97 (1992) 2948–2962.
- [32] P.V. Kamat, *Chem. Rev.* 93 (1993) 267–300.
- [33] Y. Ma, J.N. Yao, *Chemosphere* 38 (1999) 2407–2414.
- [34] J.M. Wu, T.W. Zhang, *J. Photochem. Photobiol. A* 162 (2004) 171–177.
- [35] A.J. Hoffman, E.R. Carraway, M.R. Hoffmann, *Environ. Sci. Technol.* 28 (1994) 776–785.
- [36] M.V. Rao, K. Rajeshwar, V.R. Pal Verneker, J. DuBow, *J. Phys. Chem.* 84 (1980) 1987–1991.